Inorganic Chemistry

Article

pubs.acs.org/IC

Novel Reversible Zn^{2+}-Assisted Biological Phosphate "Turn-On" Probing through Stable Aryl-hydrazone Salicylaldimine Conjugation That Attenuates Ligand Hydrolysis

Olga G. Tsay,[†] Sudesh T. Manjare,[†,‡] Hyungjun Kim,[†] Kang Mun Lee,[†] Yoon Sup Lee,[†] and David G. Churchill*,[†]

[†]Department of Chemistry, Korea Advanced Institute of Science and Technology (KAIST), 373-1 Guseong-dong, Yuseong-gu, Daejeon, 305-701, Republic of Korea

[‡]Center for Catalytic Hydrocarbon Functionalizations, Institute for Basic Science (IBS), 373-1 Guseong-dong, Yuseong-gu, Daejeon, 305-701, Republic of Korea

Supporting Information

ABSTRACT: A novel reversible zinc(II) chemosensing ensemble (**2**·Zn^{2+}) allows for selective "turn-on" fluorescence sensing of ATP and PPi in aqueous media (detection limits: 2.4 and 1.0 μM, respectively) giving selective binding patterns: ATP ~ PPi > ADP ≫ AMP > monophosphates ≈ remaining ions tested. The conjugated hydrazone [C═N—*NH*—R] resists hydrolysis considerably, compared to the imine [C═N—CH_2—R, pyridin-2-ylmethanamine] functionality, and generalizes to other chemosensing efforts. Prerequisite Zn^{2+}·[$O_{phenol}N_{imine}N_{pyr}$] binding is selective, as determined by UV−vis and NMR spectroscopy; ATP or PPi extracts Zn^{2+} to regenerate the ligand−fluorophore conjugate (PPi: turn-on, 512 nm; detection limit, 1.0 μM). Crystallography, 2-D NMR spectroscopy, and DFT determinations (B3LYP/631g*) support the nature of compound **2**. 2-Hydrazinyl-pyridine-salicylaldehyde conjugation is unknown, as such; a paucity of chemosensing-Zn^{2+} binding reports underscores the novelty of this modifiable dual cation/anion detection platform. A combined theoretical and experimental approach reported here allows us to determine both the potential uniqueness as well as drawbacks of this novel conjugation.

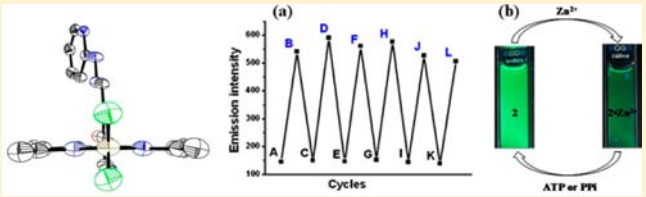

I. INTRODUCTION

Phosphates are ubiquitous in biology and play significant roles in a range of essential biological processes. They have bioenergetic roles and are involved in genome stability, lipid stability, recognition of organelle membranes, skeletal structures, protein regulation, cell signaling, and many other processes and events.[1] Nucleoside polyphosphates (*e.g.*, adenosine triphosphate, ATP, and adenosine diphosphate, ADP) constitute an important class of biological phosphates; adenosine triphosphate (ATP) is a molecule whose concentration signifies "energy currency" of intracellular energy transfer in cells and is involved in various cellular processes,[2] such as the synthesis of macromolecules (including DNA and RNA),[3] protein transport,[4] ion channel regulation,[5] and both intra- and extracellular signaling.[6] On the other hand, pyrophosphate (PPi) is the product of ATP hydrolysis and an essential anion for normal cell function. For example, PPi is involved in energy transduction mechanisms and participates in various enzymatic reactions.[7] Also, elevated PPi concentration in the synovial fluid is associated with calcium pyrophosphate dihydrate (CPPD) crystal deposition disease, and a condition termed chondrocalcinosis.[8] The roles that biological phosphates play in tubulin microtubule formation are also extremely important regarding macromolecular self-assembly essential in biology. Because of the biological importance of phosphates in living organisms, they remain the focus of various research. In recent years various detection methods have been developed; emergent and improved modalities are in high demand.[9] Fluorescence chemosensors can be designed to offer high sensitivity and rapid response to such analyte concentrations. They allow for "real-time" detection in genuine biological samples.[10] Among the various detection modes utilized for phosphate sensing, certain metal ion complexes are considered as promising molecular analytical platforms for chemical recognition under aqueous conditions.[11,12] In this context, Zn^{2+}-based sensors have been developed: they mimic metalloenzymes in their active site recognition.[13−16] Despite the intensity of this research area, few papers featuring fluorescence BODIPY−chelator·Zn^{2+} ensembles for detection of phosphates have been reported and utilized (BODIPY = boron difluorodipyrromethene, Figure 1).[17] Among the relevant known reports, a doubly substituted BODIPY with a bipyridyl unit for zinc chelation was designed. It was found to be sensitive to inorganic phosphate, but other biological polyphosphates were not tested.[17a] Dipicolylamine (DPA)

Received: May 29, 2013
Published: August 14, 2013

   dx.doi.org/10.1021/ic4013526 | *Inorg. Chem.* 2013, 52, 10052−10061

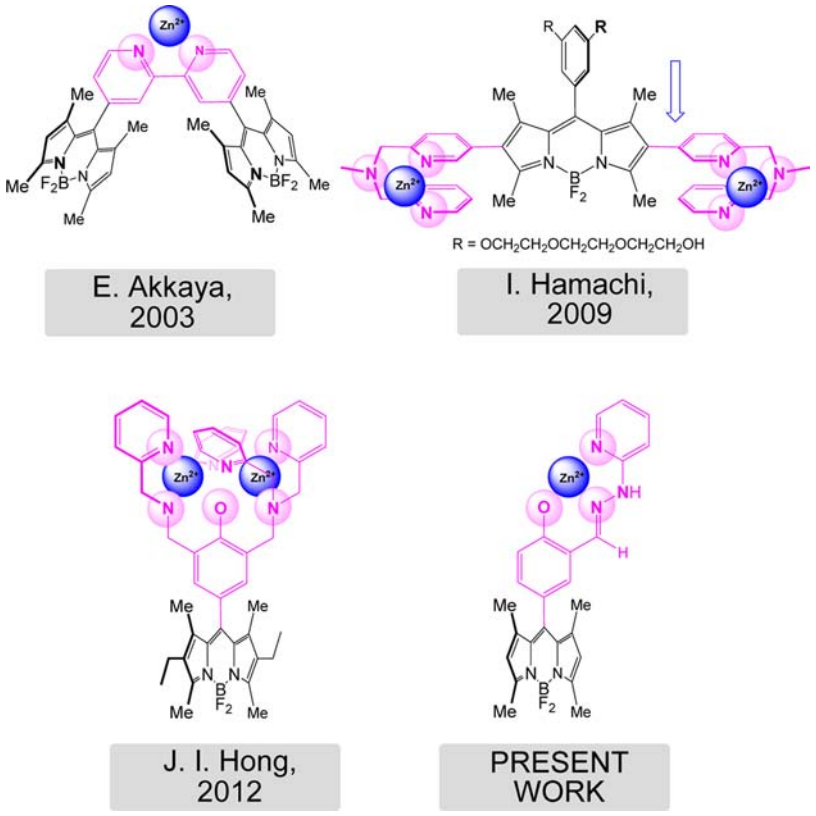

Figure 1. Structures from previous reports of BODIPY-based Zn^{2+} ensembles for phosphate sensing by, e.g., Akkaya, Hamachi, and Hong[17] and the structure pursued in the present work.

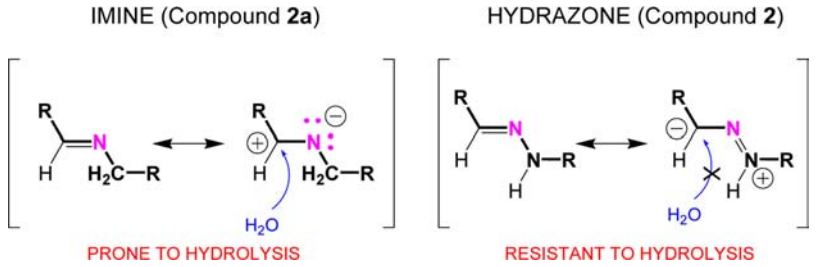

Figure 2. Differences in hydrolysis between imine and hydrazone groups.

unit was also incorporated into a BODIPY-based PPi sensor which operates *via* chemiluminescence that is generated electrically.[17b] Also, a fluorescent BODIPY-based Zn^{2+} complex was successfully utilized for the selective detection of phosphorylated tau protein in histological samples.[17c] Herein, we report a new BODIPY-Zn^{2+} ensemble for the detection of phosphates under biologically relevant conditions; a novel chelation pocket helps balance (i) cation/anion selectivity and (ii) imine hydrolysis tendencies (Figures 1 and 2). The probe was found to be sensitive to ATP and PPi when screened with other competing anion and phosphate analytes; the chelator pocket itself shows reasonable selectivity to Zn^{2+}. BODIPY–Zn^{2+} ensemble formation is possible in the presence of other interfering metal ions. Due to the strong affinity of phosphates to zinc metal ion, extraction may be effected, and fluorescence recovery, as well as probe reversibility, can be studied.[9g] There are a limited number of systems for the reversible detection of biophosphates.[12a,15a] Full characterization of the ligand has been made, and the examination of the MO patterns of this substrate via DFT geometry optimization calculations reveals important patterns pertinent to future receptor design.

Previous metal binding motifs have been explored but with limited expressed emphasis on chemosensing,[18] Zn^{2+} binding,[19] or fluorescence. The choice of hydrazinopyridine over the ubiquitous picoline-based chelations allows for the study of possible differences in solubility and hydrolysis rates.[21] The design involves a single Zn^{2+} center and a $[O_{phenol}N_{imine}N_{pyr}]$ chelation pocket along with a hydrazone linkage allowing for "greater intrinsic hydrolytic stability" via resonance stabilization (see Figure 2).[20]

II. EXPERIMENTAL SECTION

Materials and Physical Measurements. All chemicals used herein [*e.g.*, 2,4-dimethylpyrrole, 2,3-dichloro-5,6-dicyano-1,4-benzoquinone (DDQ), $BF_3{\cdot}OEt_2$, MnO_2, 2-hydrazinopyridine) were of analytical grade and used as received from commercial suppliers (Aldrich, TCI, and Junsei chemical companies]. All solvents used for spectral measurements were of analytical or HPLC grade. BODIPY compound **1** was prepared as previously reported.[21] Analytical thin layer chromatography (TLC) was performed on cuts of original plates

dx.doi.org/10.1021/ic4013526 | *Inorg. Chem.* 2013, 52, 10052−10061

Scheme 1. Synthesis for Compound 2

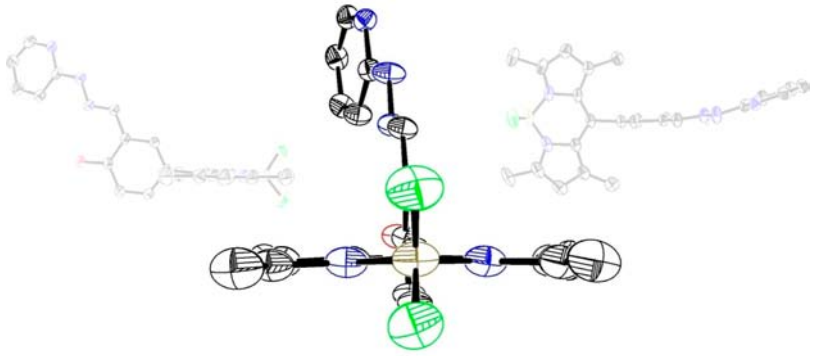

Figure 3. Front view of compound **2** as a thermal ellipsoid drawing for the crystallographic determination (for atomic numbering, see SI). "Washout" graphics of side- and top-views of the same molecular structure. Thermal ellipsoids are drawn at 30%. All hydrogen atoms are omitted for clarity. Monoclinic, $P2_1/n$, a = 10.814(2) Å, b = 14.744(3) Å, c = 16.812(3) Å, β = 96.75(3)°, V = 2662.0(9) Å^3, Z = 4.

(20 × 20 cm^2, 60 F silica gel, Merck). A Vilber Lourmat-4LC UV lamp was used to probe the fluorescence of reaction "spots" assayed by TLC (lamp: 4 W, 365 nm, 50/60 Hz). Silica gel used in column chromatography was of diameter 0.040−0.063 mm (Merck). Solvents used in NMR spectral analyses were purchased commercially and were of spectroscopy grade. ^{1}H and ^{13}C NMR spectra were recorded on a Bruker Avance 400 MHz spectrometer with TMS used as an internal standard. UV spectra were recorded with JASCO V-503 UV−vis spectrometer (1000 nm min^{-1}). Emission spectra were obtained using a SHIMADZU RF-5310 pc spectrofluorophotometer. HRMS data were obtained with a micro-TOF-QII (Bruker, Daltonik). Single-crystal X-ray data were collected on a Bruker P4 diffractometer equipped with a SMART CCD detector. The molecular structure of compound **2** was elucidated using direct methods; standard difference map techniques were used to determine the crystal structure. Full-matrix least-squares refinement procedures were performed on F2 values with the SHELXTL program (version 5.10).

Details for UV−Vis and Fluorescence Measurements. Stock solutions of **2** (1.0 mM) were prepared in absolute methanol. The 0.01 M stock solutions of metal ions (Na^+, K^+, Cs^+, Mg^{2+}, Ca^{2+}, Mn^{2+}, Fe^{2+}, Co^{2+}, Ni^{2+}, Cu^{2+}, Ag^+, Zn^{2+}, Cd^{2+}, Hg^{2+}, Pb^{2+}, and Al^{3+}) were prepared in distilled water as their perchlorate salts. Stock solutions of anions as sodium salts (F^-, Cl^-, Br^-, I^-, CH_3COO^-, CN^-, SO_4^{2-}, HCO_3^-, NO_3^-, CO_3^{2-}, $H_2PO_4^-$, HPO_4^-, $P_2O_7^{4-}$) (0.01 M) and ATP, ADP, and AMP (adenosine monophosphate) (0.01 M) were prepared in distilled water. Typically, for absorption and emission trials, test solutions were prepared by placing 15.0 μL of stock solution of **2** into a cuvette and diluting the solution to 3.0 mL with methanol/HEPES buffer solution (2:1, 0.1 M, pH = 7.2). To a solution of **2**, 10.0 equiv of metal ions were added, and emission spectra were then recorded immediately in which the excitation wavelength was set to that for the absorption maxima. Excitation and emission slit widths were 3.0 nm.

Synthesis of Compound 2. To a solution of **1** (0.04 g, 0.11 mmol) in CH_2Cl_2 (10 mL) was added 2-hydrazinopyridine (0.024 g, 0.22 mmol). The reaction mixture was refluxed for 2 h and monitored via TLC. The solvent was then removed under reduced pressure; the solid was then washed with a small amount of CH_2Cl_2 and methanol. Recrystallization from CH_2Cl_2/CH_3OH gave **2** (0.04 g) as a red powder in 80% yield. ^{1}H NMR spectral data (400 MHz, CD_2Cl_2: 5.30 ppm): δ 10.9 (br s, 1H, OH), 8.86 (br s, 1H, NH), 8.17 (d, $^3J_{H-H}$ = 5.01 Hz, 1H, H_{22}), 7.93 (s, 1H, H_{17}), 7.66 (dd, $^3J_{H-H}$ = 8.4 Hz, $^4J_{H-H}$ = 7.2 Hz, 1H, H_{20}), 7.15 (dd, $^3J_{H-H}$ = 8.1 Hz, $^4J_{H-H}$ = 2.24 Hz, 1H, H_{16}), 7.09−7.12 (m, 3H, $H_{12,15}$), 7.04 (d, $^3J_{H-H}$ = 8.4 Hz, 1H, H_{19}), 6.85 (dd, $^3J_{H-H}$ = 7.2 Hz, $^4J_{H-H}$ = 4.9 Hz, 1H, H_{21}), 6.00 (s, 2H, H_2, H_6), 2.49 (s, 6H, H_{10}), 1.48 (s, 6H, H_9). ^{13}C NMR spectral data (100 MHz, CD_2Cl_2: 54 ppm): δ 158.1 (C_{14}), 155.8 (C_{18}), 155.7 ($C_{3,5}$), 148.4 (C_{22}), 143.7 (C_{7a}), 143.7 (C_{8a}), 142.2 (C_{17}), 141.6 (C_{13}), 138.9 (C_{20}), 132.2 ($C_{1,7}$), 130.4 (C_{16}), 129.7 (C_{12}), 126.3 (C_{11}), 121.5 ($C_{2,6}$), 119.6 (C_8), 117.9 (C_{15}), 117.0 (C_{21}), 106.8 (C_{19}), 14.9 (C_{10}), 14.7 (C_9). HRMS (ESI) Calcd for $C_{25}H_{24}BF_2N_5O$: 459.2042. Found: m/z 460.2115 $(M + H)^+$.

Theoretical Calculations. A computational study was undertaken to aid the understanding of the HOMO−LUMO arrangement in compound **2** and its derivatives. Density functional theory (DFT) calculations were carried out with the Gaussian 09 program. The molecular structure of **2** was optimized using the B3LYP method together with the 631g* basis set; where applicable, the zinc atom was treated separately with the *sdd* basis set. The input coordinates for gas phase optimizations were obtained from the crystal structure coordinates. HOMO and LUMO energy levels of the molecule suggested that electron density is present over the core BODIPY molecule; for HOMO − 1 and LUMO + 1, electron density existed over the remainder of the molecule including the PET (photoinduced electron transfer) donor 2-hydrazinyl-pyridine-salicylaldehyde moiety.

Determination of Binding Constant between 2 and 2·Zn^{2+}. Binding constant was estimated by using the following equations:[30]

$$\frac{I}{I_0} = 1 + K_a[\mathrm{Zn}] \tag{1}$$

$$[\mathrm{Zn}] = \frac{1}{2}\left[\left(\mathrm{Zn}_0 - \mathrm{H}_0 - \frac{1}{K_a}\right) + \sqrt{\left(\mathrm{Zn}_0 - \mathrm{H}_0 - \frac{1}{K_a}\right)^2 + \frac{4\mathrm{Zn}_0}{K_a}}\right] \tag{2}$$

Here, H_0 is the total concentration of **2** which is considered to be constant throughout the duration of the titration; Zn_0, total

dx.doi.org/10.1021/ic4013526 | Inorg. Chem. 2013, 52, 10052−10061

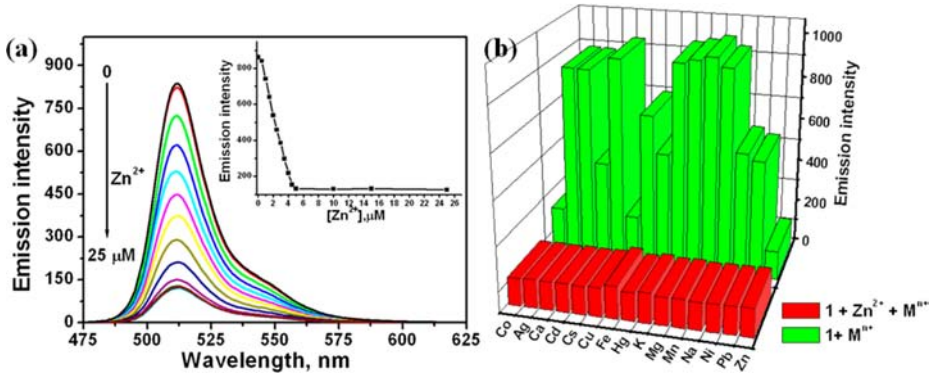

Figure 4. (a) Emission spectra of **2** (5.0 μM) upon addition of various concentrations of Zn^{2+} (0–25 μM). Inset: plot of emission intensity at 512 nm versus $[Zn^{2+}]$. (b) Competitive experiment of **2** (5.0 μM) with different metal ions in aqueous solutions (CH_3OH/HEPES buffer, 2:1, pH 7.2); λ_{emis} = 512 nm. $[M^{n+}]$ = 50 μM; $[Zn^{2+}]$ = 5 μM. λ_{ex} = 500 nm.

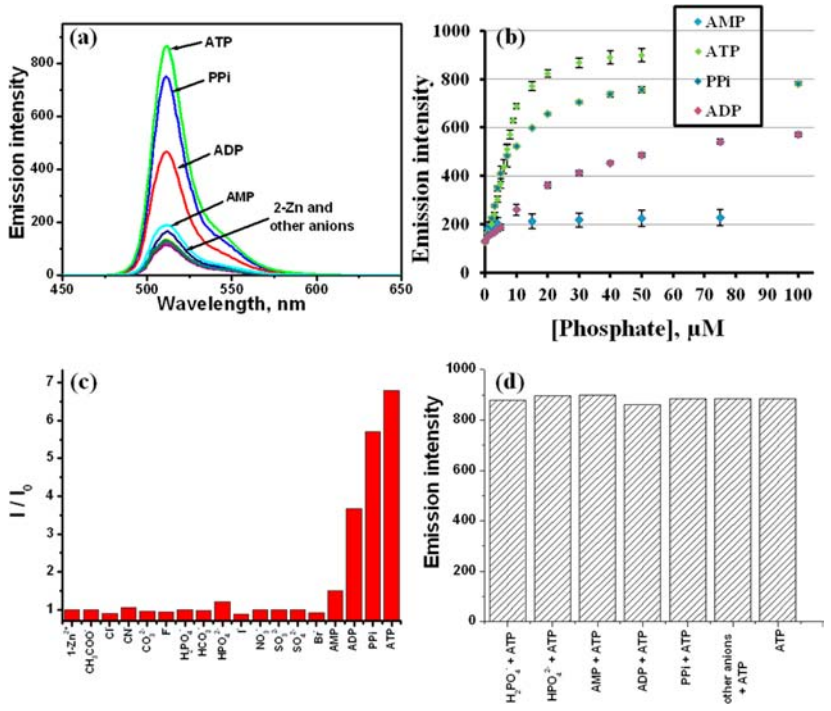

Figure 5. (a) Emission spectra of **2**·Zn^{2+} (5.0 μM) with various anions, including PPi, AMP, ADP, and ATP (50.0 μM). (b) Fluorescence titrations (in triplicate, STD) of **2**·Zn^{2+} (5.0 μM) with PPi, AMP, ADP, and ATP (0–100.0 μM). (c) Fluorescence intensity enhancement (I/I_0) of **2**·Zn^{2+} (5.0 μM) at 512 nm in the presence of different anions and AMP, ADP, and ATP (50.0 μM) in CH_3OH/HEPES buffer (2:1, pH 7.2). I_0 is the emission intensity of **2**·Zn^{2+}. (d) Emission intensity at 512 nm of **2**·Zn^{2+}·ATP in the presence of different anions: [**2**·Zn] = 5.0 μM, [ATP] = [anions] = 50.0 μM. Conditions: CH_3OH/:HEPES buffer (2:1, pH 7.2); λ_{em} = 512 nm, λ_{ex} = 500 nm.

concentration of added Zn^{2+}; K_a, binding constant; [Zn], concentration of the free Zn^{2+} in the equilibrium.

Determination of Stoichiometry and Binding Constant for ATP and PPi Binding with 2·Zn^{2+}. The interaction between **2**·Zn^{2+} and polyphosphates was analyzed according to the Benesi–Hildebrand equation for spectrofluorometric titration:[28]

$$\frac{I_0}{I_0 - I} = A + \frac{B}{K_a[\text{analyte}]^2}$$

Here, K_a, I_0, and I are, respectively, the binding constant, the observed fluorescence intensity (in the absence of analyte), and the observed fluorescence intensity (in the presence of analyte). Binding constants were estimated from titration experiments as the ratio between the *y*-intercept and the slope of the linear "best fit."

III. RESULTS AND DISCUSSION

Synthesis. BODIPY **2** was synthesized from the previously reported compound **1**[21] through the addition of 2-hydrazinopyridine in methylene chloride under reflux (Scheme 1). Detailed synthetic procedures and characterization data are provided in the Experimental Section. Also, a single-crystal X-ray structure was obtained (Figure 3). Compound **2** was characterized by ^1H and ^{13}C NMR spectroscopy and ESI-HRMS.

Compound **2** was found in the $P2_1/n$ space group in a crystal grown from a CH_2Cl_2/CH_3OH solvent mixture. There is no solvent of crystallization. Structurally, the expected 2-hydroxy-2-(2-pyridinyl)hydrazone benzaldehyde-based *meso* group is present: the *meso* group–BODIPY rotor angle was found to be ~89°. The hydrazone group is effectively coplanar (non-H

dx.doi.org/10.1021/ic4013526 | Inorg. Chem. 2013, 52, 10052–10061

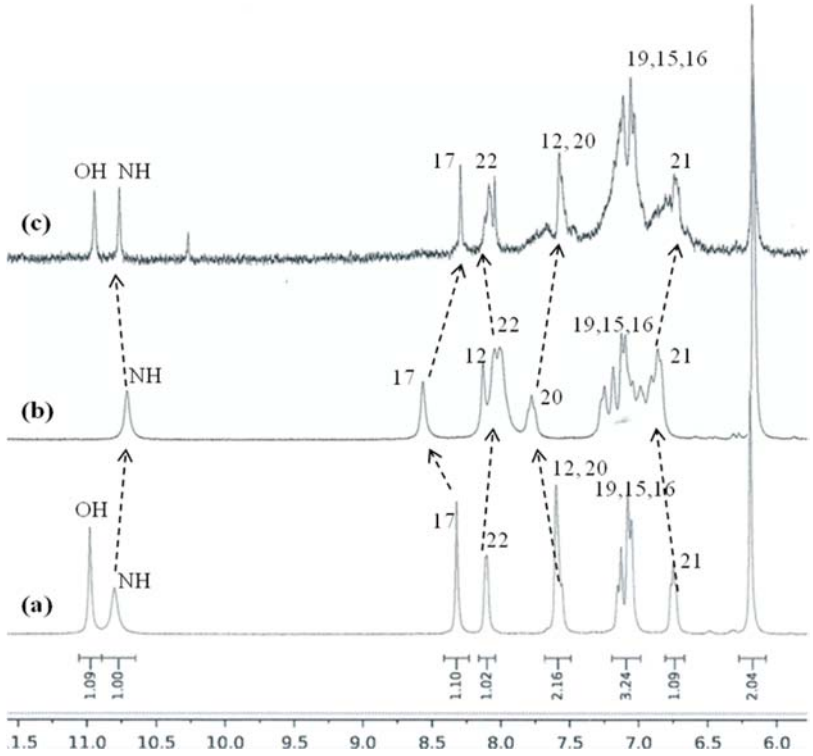

Figure 6. ^{1}H NMR spectrum for (a) **2** in DMSO; (b) **2** in the presence of 1.2 equiv of Zn^{2+}, to give **2**·Zn^{2+}·nH_2O; and (c) **2** in the presence of 1.2 equiv Zn^{2+} and 2.0 equiv of PPi (relative to Zn^{2+}) to give **2**·Zn^{2+}·PPi. [**2**] = 0.02 M.

mean-plan deviation: 0.16). The imine C_{17}−N bond length is 1.28 Å; the N−C_{18} bond length is 1.38 Å. The N−N bond length is 1.37 Å; the C_{13}−C_{17} bond length is 1.46 Å, consistent with element−element single bonds. The *ortho*-N_{py} is rotated distal from the hydroxyl group. Also, the entire 8-substituent has a bent countour (Figure 3). The deviation in the BODIPY mean plane is minimal (0.024 Å); alternate C═C and C—C bond lengths are clearly evident.

Formation of BODIPY−Zn^{2+} Ensemble. Compound **2** has moderate fluorescence under aqueous conditions (Φ_F = 0.27 ± 0.01;[22] CH_3OH/HEPES buffer, 2:1, pH 7.2). However, in the presence of Zn^{2+} (5.0 μM), the fluorescence of **2** drops dramatically (Φ_F = 0.038 ± 0.002) (Figure 4). Other metal ions (Na^+, K^+, Cs^+, Mg^{2+}, Ca^{2+}, Mn^{2+}, Fe^{2+}, Co^{2+}, Ni^{2+}, Cu^{2+}, Ag^+, Zn^{2+}, Cd^{2+}, Hg^{2+}, Pb^{2+}, Al^{3+}) were also examined. A decrease of emission intensity was observed in the presence of Co^{2+}, Cu^{2+}, Cd^{2+}, and to a lesser extent Hg^{2+}, Pb^{2+}, Fe^{2+}, Ni^{2+} (Figure S10). While these reductions in fluorescence were not as dramatic as those found for Zn^{2+} they cannot be ignored as potential competitors for the Zn^{2+}. After equilibration was established in these standard competntiion-type reactions, when Zn^{2+} and a competitor both show a decrease in fluorescence intensity, it requires careful work to determine the extent of mixing. In the worst case, such interference may be inconclusive. Interestingly, Cd^{2+}, a common interferent in Zn^{2+} sensing, gives only a moderate change in fluorescence intensity for **2**. When 10 equiv of various competitive metal ions were assayed, in the case of Zn^{2+}, only 1 equiv was enough to "turn off" the emission. Additionally, competitive experiments revealed that Zn^{2+} complexation is predominant in the presence of other metal ions (Figure 4b), even with Cu^{2+}.

Fluorescence titration experiments for **2** (5.0 μM) with different concentrations of Zn^{2+} show gradual decreases in emission intensity; saturation is reached with 1.0 equiv of Zn^{2+} signifying the formation of the **2**·Zn^{2+} complex (Figure 4). For 1:1 binding stoichiometry, a binding constant of $K_a = 1.1 \times 10^7$ M^{-1} was obtained (Figure S12). The formation of the zinc complex was also tracked by mass spectrometry (HRMS) (Figure S6). The peak at 522.1260 corresponds to a 1:1 complex formation $[C_{25}H_{24}BF_2N_5O + Zn]^+$, consistent with the calculated m/z mass value of 522.1255.

Sensing of Polyphosphates with a BODIPY−Zn^{2+} Ensemble. As the **2**·Zn^{2+} ensemble is weakly fluorescent, the sensing ability of this system toward various anions, including biological phosphates, was evaluated by further fluorescence spectroscopic measurements. The zinc complex **2**·Zn^{2+} (5.0 μM) was prepared *in situ* and treated with various anions including F^-, Cl^-, Br^-, I^-, CH_3COO^-, CN^-, SO_4^{2-}, HCO_3^-, NO_3^-, CO_3^{2-}, $H_2PO_4^-$, HPO_4^{2-}, $P_2O_7^{4-}$ (PPi), as well as ATP, ADP, and AMP. Figure 5 clearly shows that **2**·Zn^{2+} is highly sensitive to polyphosphates PPi and ATP. The emission intensity of the **2**·Zn^{2+} ensemble increases upon addition of ATP and PPi; the other anions, including inorganic phosphates and AMP, give no observable changes. Interestingly, ADP gives moderate emission changes. Fluorescence titration profiles of **2**·Zn^{2+} (5.0 μM) with different concentrations of polyphosphates (0−100.0 μM) indicate that fluorescence intensity increases gradually with increasing concentration of polyphosphates and reaches saturation at ∼20 μM for ATP and PPi, constituting ∼95% and ∼70%, of the fluorescence signal for **2**, respectively (Figure 5b). Since the addition of ATP and PPi gives a recovery of fluorescence identical to that for **2**, we propose that the mechanism of sensing involves initial bidentate binding of one phosphate to **2**·Zn^{2+} (see Figure 9) followed by the full displacement of zinc ion by a second chelating polyphosphate. Binary-type compounds [Zn^{2+}·2PPi] or [Zn^{2+}·2ATP] would thus form, liberating compound **2**. The decomplexation of zinc ion by polyphosphates has been previously reported, but

dx.doi.org/10.1021/ic4013526 | *Inorg. Chem.* 2013, 52, 10052−10061

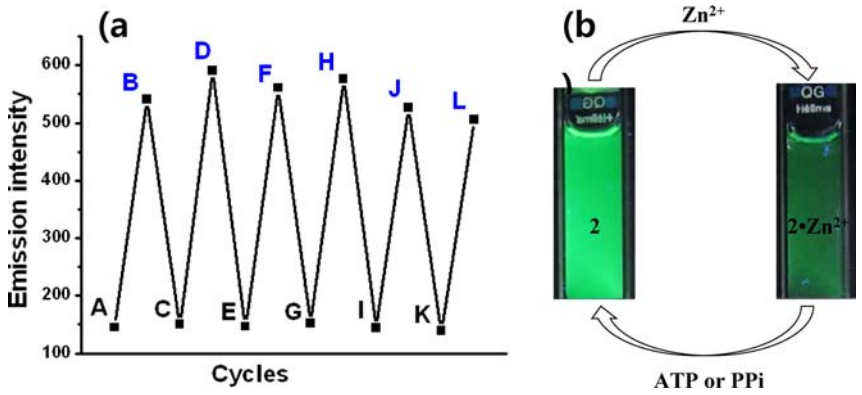

Figure 7. (a) Fluorescence experiments showing significant and reversible "on−off" responses for the detection of PPi by **2**·Zn^{2+}. [**2**] = [Zn^{2+}] = 5.0 μM, [PPi] = 10 μM; A = **2**·Zn^{2+}, B = A + [PPi], C = B + [Zn^{2+}], D = C + [PPi], E = D + [Zn^{2+}], F = E + [PPi], G = F + [Zn^{2+}], H = G + [PPi], I = H + [Zn^{2+}], J = I + [PPi], K = J + [Zn^{2+}], L = K + [PPi]. (b) Photographs of **2** (5.0 μM) and **2**·Zn^{2+} (5.0 μM) under UV excitation (365 nm), [ATP] = 10 μM.

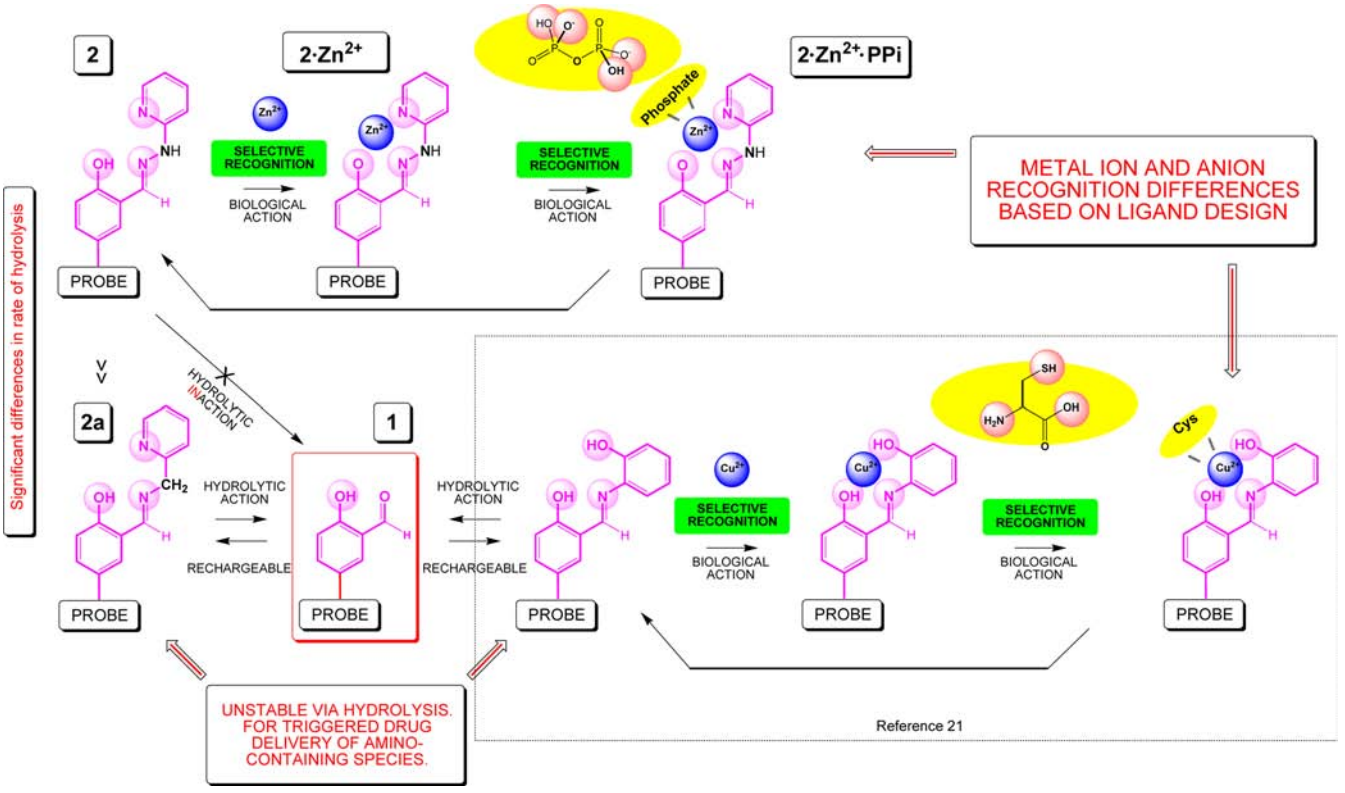

Figure 8. Summary of hydrolytic pathways for probe **2**·Zn^{2+} and related systems.[21]

stepwise mechanistic studies are absent,[15a,23] thus spurring an entry into theoretical calculations shown below (Figure 9) as well as mass spectrometric studies.

Fluorescence spectra confirm that for the total release of **2** from **2**·Zn^{2+}, 2.0 equiv of ATP or PPi is required, leading to a proposed 1:2 interaction between **2**·Zn^{2+} and polyphosphate, supported by Benesi−Hildebrand analysis (Figure S13). At 2.0 equiv of analyte loading, it is proposed that phosphate binding out-competes core [$O_{phenol}N_{imine}N_{pyr}$] binding leading to the liberation of **2** and proposed formation of a Zn^{2+}·2PPi type species. Estimated binding constants for ATP and PPi were determined on the basis of this ratio (Figure S13). Detection limits for ATP and PPi were evaluated as 2.4 and 1.0 μM, respectively (Figure S14), much lower than that concentrations found in cells.[29] Also, ATP sensing by **2**·Zn^{2+} is possible in the presence of other anions, including phosphates, such as HPO_4^{2-}, $H_2PO_4^-$, AMP, and ADP (Figure 5d).

To further confirm the binding mode and to support the proposed mechanism, NMR spectroscopic titrations and MS studies were carried out. An ^{1}H NMR tube experiment was performed and supports the occurrence of a clean complexation event of **2** with Zn^{2+} giving the downfield spectral shift for (or complete removal of) signals assigned to protons of neighboring groups: hydrazone (8.23 → 8.57 ppm), pyridyl ($\Delta\delta$ = 0.22 and 0.12 ppm), and phenol (see Figure 6). Small upfield shifts for the NH and H_{22} protons were also detected. This experiment further supports phenolic-, pyridyl-, and hydrazonyl-Zn2+ binding, in which the [$N_{aniline}$] group is directed away (Figure 1). After the addition of 2 equiv of PPi to **2**·Zn^{2+}, the ^{1}H NMR spectra resembles that formed for **2**,

dx.doi.org/10.1021/ic4013526 | Inorg. Chem. 2013, 52, 10052−10061

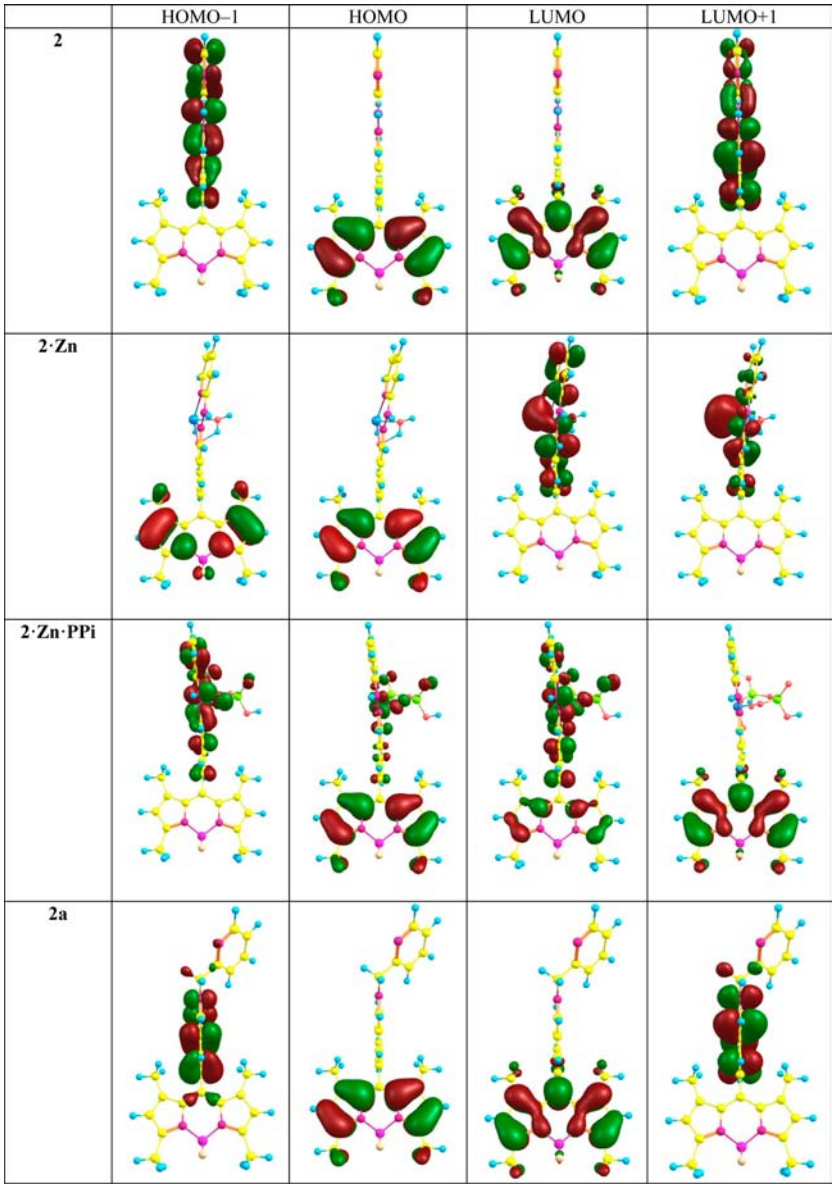

Figure 9. HOMO − 1, HOMO, LUMO, and LUMO + 1 (from left to right) of geometry-optimized molecules **2**, **2**·Zn^{2+}, **2**·Zn^{2+}·PPi, and **2a** (from top to bottom) in gas phase calculations (B3LYP method and 631g* basis set; *sdd* basis set for the zinc atom).

indicating a complete dissociation of Zn^{2+} from **2**, enabled by the strong competitive chelating action of multiple equivalents of PPi.

Mass spectrometry provides additional support for the liberation of **2**. These spectra (Figure S7) reveal values consistent with zinc-bound PPi species along with a peak corresponding to **2** in independent form.[24] Also, a mass peak consistent with the formation of complex [**2** + Zn + PPi] was observed; here, a *m*/*z* peak of 803.2391 was assigned as [**2** + Zn + PPi + $2H_2O$ + 3Na + H]$^+$. Thus, a mechanism involving the binding of polyphosphate to **2**·Zn^{2+}, with subsequent removal of Zn^{2+} from **2**·Zn^{2+} and release of **2**, is further supported.

Reversibility, Hydrolysis, and Context of Chemosensing Action. Reversibility and hydrolytic action are important criteria in chemosensing, especially when the hydration sphere of the metal ion is considered. Since the detection mode is based on the removal of the Zn^{2+} from **2**·Zn^{2+} by phosphates, probe reversibility was tested *via* PPi titrations. When PPi (2 equiv) was added to **2**·Zn^{2+}, the fluorescence intensity is increased. Further addition of Zn^{2+} resulted in the recovery of emission intensity suggesting the *in situ* reformation of **2**·Zn^{2+}. The cycle can be repeated with alternate fluorescence "turn-on", "turn-off" behavior clearly observed beyond 5 cycles of repetition (Figure 7).

The chelator design in **2** is minimal, compared to that for the conjugate reported by Hong and co-workers. In fact, our 4-phenoxy and neighboring 3-substituent position are borrowed motifs. Importantly, potential Schiff base hydrolysis is surmounted by the presence of the hydrazone group; sensor **2** does not produce the bare salicylaldehyde derivative (**1**) (Figure 8). 2,2′-Dipicolylamine (DPA) is a well-known binding moiety for zinc ion, and many zinc sensors based on 2,2′-dipicolylamine (DPA)[13] and Zn^{2+}−DPA complexes for phosphate sensing have already been developed.[13,16,25] Importantly, the 2-picolylamine Schiff base version of compound **2** was also prepared for comparison (Supporting Information); however, the ligand is highly unstable toward hydrolysis under aqueous conditions thus precluding sub-

dx.doi.org/10.1021/ic4013526 | *Inorg. Chem.* 2013, 52, 10052−10061

sequent Zn^{2+} complex formation studies (Figure S8).[21] For **2**·Zn^{2+}, this hydrolytic pathway is suppressed for hydrazone **2** (based on resonance stabilization, *vide infra*). The hydrazone bond in **2** under aqueous conditions and Zn^{2+}-complexes[26] is stable[20] and can be easily prepared and used further for sensing of biologically relevant analytes. This motif can become a general design parameter in metal-ion-based chemosensing. What makes **2** important and largely different in utility from those shown in Figure 1 is its demonstrated ability to operate with cations *and* anions that are both biorelevant in nature. The hydrolytic differences of ligand **2**, compound **1**, and related systems and their fluorescence capacities are summarized above (Figure 8). There is also a relationship to salicylaldehyde itself, determined to be of low neurotoxicity, and relevant to biology and proteins.[27] Additionally, the general lack of toxicity of BODIPY is encouraging when pursuing conjugates such as compound **1**. The ensemble is different enough from closely related systems (Figure 1): **2** itself leads to fluorescence enhancement and resists hydrolysis. In a related case, **1** does form.[21] But, with 2-(2-pyridinyl)hydrazone benzaldehyde conjugation, generation of probe **2** is retained cleanly, enabling cycling as shown (Figure 7).

Computational HOMO−LUMO Analysis. Geometry optimizations of **2**, **2**·Zn^{2+}, and **2**·Zn^{2+}·PPi were undertaken. Structural parameters and coordinates were used, and the generation of frontier molecular orbital depictions and their relative electronic energies were obtained. HOMO/LUMO comparisons were made with ligand **2** (Figure 9). Subsequent to this, and on the basis of geometries of closely related structural fragments, structures of **2**·$Zn^{2+}(H_2O)_2$ and **2**·Zn^{2+}PPi were successfully optimized and assessed electronically (see Table 1 and SI). An assessment of very different electronic distributions in LUMO and LUMO + 1 levels suggest the origin of the donor−acceptor dyad. In the LUMO + 1 diagram, the donor group is clearly blanketed by electron density. Furthermore, geometric features, such as those found for the crystal structure, are retained: the calculated imine bond length is 1.29 Å (versus 1.28 Å determined from X-ray structural data); the N−C_{18} bond length is 1.39 Å; the N−N bond length is 1.34 Å; finally, the C_{13}−C_{17} bond length is 1.45 Å. Structural values, respectively, of 1.38, 1.37, and 1.46 Å show accord between theory and experiment. The HOMO levels in both **2** and **2**·Zn^{2+} are localized mainly on the BODIPY fluorophore. However, differences exist at the LUMO level. For compound **2**, the LUMO is localized on the fluorophore core, whereas the LUMO of the zinc complex is located on the hydrazone moiety. A complete HOMO → LUMO photoexcited electron transfer mechanism is therefore proposed. Further, addition of PPi leads to a delocalization of electron density from the zinc binding site to the BODIPY fluorophore; here, the nonfluorescent nature of the zinc complex has been incapacitated allowing for a redistribution of electron density which causes an increase in fluorescence. The imine version was also studied via calculations in which the [NH] unit was formally switched to a [CH_2] unit (**2a**), despite the experimentally observed lack of hydrolytic stability. Aside from the HOMO − 1, the HOMO−LUMO differences are very similar (Table 1). Next, the metal center environment of both the **2**·Zn^{2+}·$(H_2O)_2$ and **2**·Zn^{2+}·PPi is square pyramidal; in **2**·Zn^{2+}·$(H_2O)_2$, bound water hydrogens were reached by proximal heteroatoms in a small hydrogen-bonding network.

Table 1. Relative Energy Levels (eV) for Compounds 2, 2·Zn^{2+}, and 2·Zn^{2+}·PPi

	2 (**2a**)	**2**·Zn^{2+}·$2H_2O$	**2**·Zn^{2+}·PPi
LUMO + 1	3.66 (3.64)	2.69	2.98
LUMO	2.99 (3.00)	2.17	0.39
HOMO	0.00	0.00	0.00
HOMO − 1	−0.33 (−0.91)	−1.14	−0.42

IV. CONCLUSION

In conclusion, we report a new hydrolysis-resistant zinc-ion-based detection modality for biological polyphosphate binding/detection. Herein, a specific BODIPY-conjugate for selective "turn-on" fluorescence sensing of pyrophosphate and ATP at a single Zn^{2+} center was demonstrated in aqueous media. The sensing mode involves demetalation of the weakly fluorescent **2**·Zn^{2+} by ATP and PPi, leading to fluorescence enhancement due to production of the fluorescent compound **2**. The probe ensemble shows competitive selectivity for ATP and PPi over other anions, including inorganic phosphates. The ensemble is different from previous closely related systems: the production of **2**, and not **1**, dictates adequate fluorescence enhancement, and importantly demonstrates clean optical signal cycling via Zn^{2+}/PPi addition. Detection limits were estimated on the order of micromolar concentration: 2.4 μM for ATP and 1.0 μM for PPi, lower than levels found biologically. Probe **2** was not explicitly considered in the detection of Zn^{2+} in its own right (turn-off), but is selective as demonstrated when Zn^{2+} is held in competition with various other metal ions. The picoline version (pyridin-2-ylmethanamine) hydrolyzes readily upon ligand synthesis and is thus not practical for tandem metal ion−anion screening. Substitution at **2** by aryl amino groups is subtle: (i) imine bonds are vulnerable upon Schiff base formation; (ii) heteroatom placements steer metal ion/anion binding/recognition; (iii) metal·*n*(anion) fragment dissociation leads to probe **2** liberation. The probe is reversible: after binding with PPi or ATP, **2**·Zn^{2+} can be easily regenerated by the addition of Zn^{2+} *in situ*. Triggered drug delivery and concepts in molecular neurodegenerative disease research will be pursued in future work.

■ ASSOCIATED CONTENT

Supporting Information

Crystallographic data in CIF format. Synthesis, characterization, and spectroscopic and binding studies of **2** and **2**·Zn^{2+} with phosphates. This material is available free of charge via the Internet at http://pubs.acs.org. The CIF data of crystallographic determinations have also been deposited with the Cambridge Crystallographic Data center. These data are available at www.ccdc.cam.ac.uk/conts/retrieving.html or from the CCDC, 12 Union Road, Cambridge CB2 IEZ, United Kingdom. E-mail: deposit@ccdc.cam.ac.kr.

■ AUTHOR INFORMATION

Corresponding Author

*E-mail: dchurchill@kaist.ac.kr. Phone: +82-42-350-2845. Fax: +82-42-350-2810.

Notes

The authors declare no competing financial interest.

■ ACKNOWLEDGMENTS

The Molecular Logic Gate Laboratory (D.G.C.) acknowledges research support from the National Research Foundation (NRF) (Grants 2011-0017280, 2010-0013660, 2009-0070330). S.T.M. acknowledges support from Institute for Basic Science (IBS) for his postdoctoral fellowship. Mr. Hack Soo Shin and Prof. Youngkyu Do are acknowledged, respectively, for facilitating the acquisition of NMR spectroscopic and crystallographic data. The research support staff at KAIST facilitated the acquisition of MS data.

■ REFERENCES

(1) (a) Hirsch, A. K. H.; Fischer, F. R.; Diederich, F. *Angew. Chem., Int. Ed.* **2007**, *46*, 338−352. (b) Bowler, M. W.; Cliff, M. J.; Waltho, J. P.; Blackburn, G. M. *New J. Chem.* **2010**, *34*, 784−794.

(2) Berg, J. M.; Tymoczko, J. L.; Stryer, L. *Biochemistry*, 5th ed.; W. H. Freeman and Company: New York, 2002.

(3) (a) Stubbe, J. *J. Biomol. Chem.* **1990**, *265*, 5329−5332. (b) Shen, X.; Mizuguchi, G.; Hamiche, A.; Wu, C. *Nature* **2000**, *406*, 541−544. (c) Kornberg, A. *J. Biol. Chem.* **1988**, *263*, 1−4.

(4) Eckford, P. D. W.; Sharom, F. J. *Chem. Rev.* **2009**, *109*, 2989−3011.

(5) (a) Blanco, G.; Mercer, R. W. *Am. J. Physiol.* **1998**, *275*, F633−F650. (b) Ashcroft, F. M.; Gribble, F. M. *Diabetologia* **1999**, *42*, 903−919.

(6) Burnstock, G. *Pharmacol. Rev.* **2006**, *58*, 58−86.

(7) (a) Wilcox, D. E. *Chem. Rev.* **1996**, *96*, 2435−2458. (b) Cleland, W. W.; Hengge, A. C. *Chem. Rev.* **2006**, *106*, 3252−3278.

(8) Doherty, M.; Belcher, C.; Regan, M.; Jones, A.; Ledingham, J. *Ann. Rheum. Dis.* **1996**, *55*, 432−436.

(9) (a) Liu, X.; Ngo, H. T.; Ge, Z.; Butler, S. J.; Jolliffe, K. A. *Chem. Sci.* **2013**, *4*, 1680−1686. (b) Butler, S. J.; Jolliffe, K. A. *Chem.—Asian J.* **2012**, *7*, 2621−2628. (c) Ambrosi, G.; Formica, M.; Fusi, V.; Giorgi, L.; Guerri, A.; Macedi, E.; Micheloni, M.; Paoli, P.; Pontellini, R.; Rossi, P. *Inorg. Chem.* **2009**, *48*, 5901−5912. (d) Nonaka, A.; Horie, S.; James, T. D.; Kubo, Y. *Org. Biomol. Chem.* **2008**, *6*, 3621−3625. (e) Chen, Z.-h.; Lu, Y.; He, Y.-b.; Huang, X.-h. *Sens. Actuators, B* **2010**, *149*, 407−412. (f) Lee, D.-N.; Jo, A.; Park, S. B.; Hong, J.-I. *Tetrahedron Lett.* **2012**, *53*, 5528−5530. (g) Kim, K.; Ha, Y.; Kaufman, L.; Churchill, D. G. *Inorg. Chem.* **2012**, *51*, 928−938.

(10) Valeur, B. *Molecular Fluorescence: Principles and Applications*; Wiley−VCH: Weinheim, 2002.

(11) (a) O'Neil, E. J.; Smith, B. D. *Coord. Chem. Rev.* **2006**, *250*, 3068−3080. (b) Beer, P. D.; Gale, P. A. *Angew. Chem., Int. Ed.* **2001**, *40*, 486−516. (c) Martinez-Máñez, R.; Sancenón, F. *Chem. Rev.* **2003**, *103*, 4419−4476.

(12) (a) Deng, J.; Yu, P.; Yang, L.; Mao, L. *Anal. Chem.* **2013**, *85*, 2516−2522. (b) Shao, N.; Jin, J.; Wang, G.; Zhang, Y.; Yang, R.; Yuan, J. *Chem. Commun.* **2008**, *9*, 1127−1129. (c) Ganjali, M. R.; Hosseini, M.; Aboufazeli, F.; Faridbod, F.; Goldooz, H.; Badiei, A. R. *Luminescence* **2012**, *27*, 20−23.

(13) (a) Xu, Z.; Yoon, J.; Spring, D. R. *Chem. Soc. Rev.* **2010**, *39*, 1996−2006. (b) Lee, H. N.; Xu, Z.; Kim, S. K.; Swamy, K. M. K.; Kim, Y.; Kim, S.-J.; Yoon, J. *J. Am. Chem. Soc.* **2007**, *129*, 3828−3829.

(14) Reported selective systems for ATP: (a) Kaur, J.; Singh, P. *Chem. Commun.* **2011**, *47*, 4472−4474. (b) Rao, A. S.; Kim, D.; Nam, H.; Jo, H.; Kim, K. H.; Ban, C.; Ahn, K. H. *Chem. Commun.* **2012**, *48*, 3206−3208. (c) Strianese, M.; Milione, S.; Maranzana, A.; Grassi, A.; Pellecchia, C. *Chem. Commun.* **2012**, *48*, 11419−11421. (d) Ojida, A.; Miyahara, Y.; Wongkongkatep, J.; Tamaru, S.-i.; Sada, K.; Hamachi, I. *Chem.—Asian J.* **2006**, *1*, 555−563. (e) Kurishita, Y.; Kohira, T.; Ojida, A.; Hamachi, I. *J. Am. Chem. Soc.* **2012**, *134*, 18779−18789. (f) Kaur, J.; Singh, P. *Chem. Commun.* **2011**, *47*, 4472−4474. (g) Moro, A. J.; Cywinski, P. J.; Körsten, S.; Mohr, G. J. *Chem. Commun.* **2010**, *46*, 1085−1087. (h) Kurishita, Y.; Kohira, T.; Ojida, A.; Hamachi, I. *J. Am. Chem. Soc.* **2010**, *132*, 13290−13299. (i) Xu, Z.; Singh, N. J.; Lim, J.; Pan, J.; Kim, H. N.; Park, S.; Kim, K. S.; Yoon, J. *J. Am. Chem. Soc.* **2009**, *131*, 15528−15533.

(15) Selective for PPi: (a) Pathak, R. K.; Rai, A.; Panda, D.; Rao, C. P. *Anal. Chem.* **2012**, *84*, 5117−5123. (b) Ravikumar, I.; Ghosh, P. *Inorg. Chem.* **2011**, *50*, 4229−4231. (c) Shao, N.; Wang, H.; Gao, X.; Yang, R. H.; Chan, W. H. *Anal. Chem.* **2010**, *82*, 4628−4636. (d) Lee, D. H.; Kim, S. Y.; Hong, J.-I. *Angew. Chem., Int. Ed.* **2004**, *43*, 4777−4780. (e) Cho, H. K.; Lee, D. H.; Hong, J.−I. *Chem Commun* **2005**, 1690−1692. (f) Kim, S. K.; Lee, D. H.; Hong, J.−I.; Yoon, J. *Acc. Chem. Res.* **2009**, *42*, 23−31. (g) Wen, J.; Geng, Z.; Yin, Y.; Zhang, Z.; Wang, Z. *Dalton Trans.* **2011**, *40*, 1984−1989. (h) Roy, B.; Rao, A. S.; Ahn, K. H. *Org. Biomol. Chem.* **2011**, *9*, 7774−7779. (i) Rao, A. S.; Singh, S.; Choi, W.; Ahn, K. H. *Org. Biomol. Chem.* **2012**, *10*, 8410−8417. (j) Chen, W.−H.; Xing, Y.; Pang, Y. *Org. Lett.* **2011**, *13*, 1362−1365. (k) Zhang, J. F.; Kim, S.; Han, J. H.; Lee, S.-J.; Pradhan, T.; Cao, Q. Y.; Lee, S. J.; Kang, C.; Kim, J. S. *Org. Lett.* **2011**, *13*, 5294−5297.

(16) Sakamoto, T.; Ojida, A.; Hamachi, I. *Chem. Commun.* **2009**, 141−152 and references therein.

(17) (a) Coskun, A.; Baytekin, B. T.; Akkaya, E. U. *Tetrahedron Lett.* **2003**, *44*, 5649−5651. (b) Shin, I.-S.; Bae, S. W.; Kim, H.; Hong, J.-I. *Anal. Chem.* **2010**, *82*, 8259−8265. (c) Ojida, A.; Sakamoto, T.; Inoue, M.; Fujishima, S.-h.; Lippens, G.; Hamachi, I. *J. Am. Chem. Soc.* **2009**, *131*, 6543−6548.

(18) (a) Meng, Z.-S.; Guo, F.-S.; Liu, J.-L.; Leng, J.-D.; Tong, M.-L. *Dalton Trans.* **2012**, *418*, 2320−2329. (b) Larionov, S. V.; Savel'eva, Z. A.; Klevtsova, R. F.; Uskov, E. M.; Glinskaya, L. A.; Popov, S. A.; Tkachev, A. V. *Russ. J. Coord. Chem.* **2011**, *37*, 1−7. (c) Ghosh, K.; Kumar, P.; Tyagi, N.; Singh, U. P. *Inorg. Chem.* **2010**, *49*, 7614−7616. (d) Hosny, N. M.; Mahmoud, M. A.l-M.; Aly, M. R. E. *Synth. React. Inorg., Met.-Org., Nano-Met. Chem.* **2010**, *40*, 439−446. (e) Enomoto, K. Jpn. Kokai Tokkyo Koho JP 2004134289 A 20040430, 2004. (f) Swamy, S. J.; Reddy, S. R. *Indian Chem., Sect. A* **2001**, *40A*, 1093−1096. (g) Chia, L. M. L.; Wheatley, A. E. H.; Feeder, N.; Davies, J. E.; Halcrow, M. A. *Polyhedron* **2000**, *19*, 109−114. (h) Vecchio-Sadus, A. M. *Trans. Met. Chem.* **1995**, *20*, 256−61. (i) Mohan, M.; Gupta, N. S.; Chandra, L.; Jha, N. K. *J. Inorg. Biochem.* **1987**, *31* (1), 7−27. (j) Anderson, R. G.; Nickless, G. *Talanta* **1967**, *14* (11), 1221−8.

(19) For reports about 2-(2-pyridinyl)hydrazone benzaldehyde and sensors see: (a) Gong, Z.-L.; Ge, F.; Zhao, B.-X. *Sens. Actuators, B* **2011**, *159*, 148−153. (b) Panchal, R. G.; Kota, K. P.; Spurgers, K. B.; Ruthel, G.; Tran, J. P.; Boltz, R. C.; Bavari, S. *J. Biomol. Screening* **2010**, *15* (7), 755−765.

(20) Kalia, J.; Raines, R. T. *Angew. Chem., Int. Ed.* **2008**, *47*, 7523−7526.

(21) Tsay, O. G.; Lee, K. M.; Churchill, D. G. *New J. Chem.* **2012**, *36*, 1949−1952.

(22) Average molecular fluorescence quantum yields are provided from triplicate measurements determined in CH_3OH. See, *e.g.* : Demas, , J. N. In *Optical Radiation Measurements*; Mielenz, , K. D., Ed.; Academic Press: New York, **1982**,; Vol. 3, (Measurement of Photoluminescence), pp 195−248.

(23) (a) Wezenberg, S. J.; Anselmo, D.; Escudero-Adan, E. C.; Buchholz, J. B.; Kleij, A. J. *Eur. J. Inorg. Chem.* **2010**, *29*, 4611−4616. (b) Wezenberg, S. J.; Anselmo, D.; Escudero-Adan, E. C.; Benet-Buchholz, J.; Kleij, A. J. *Org. Lett.* **2008**, *10*, 3311−3314. (c) Wild, A.; Winter, A.; Hager, M. D.; Schubert, U. S. *Analyst* **2012**, *137*, 2333−2337.

(24) The m/z value of 499.1907 constitutes $[\mathbf{2}\cdot PPi + Zn + 2H_2O + 2Na^+ + 4H]^+$. The m/z value of 543.1539 is assigned to a product including $Zn\cdot PPi_2$: $[\mathbf{2}\cdot PPi + Zn + 2H_2O + 4Na^+ + 2H]^+$. The peak at 515.1551 corresponds to free **2**: $[\mathbf{2} + Na + CH_3OH + H]^+$.

(25) (a) Oh, J.; Hong, J.-I. *Org. Lett.* **2013**, *15*, 1210−1213. (b) Rhee, H.-W.; Choi, S. J.; Yoo, S. H.; Jang, Y. O.; Park, H. H.; Pinto, R. M.; Cameselle, J. C.; Sandoval, F. J.; Roje, S.; Han, K.; Chung, D. S.; Suh, J.; Hong, J.-I. *J. Am. Chem. Soc.* **2009**, *131*, 10107−10112. (c) Ngo, H. T.; Liu, X.; Jolliffe, K. A. *Chem. Soc. Rev.* **2012**, *41*, 4928−4965.

(26) Cao, J.; Zhao, C.; Wang, X.; Zhang, Y.; Zhu, W. *Chem. Commun.* **2012**, *48*, 9897−9899.

(27) Ha, Y.; Liew, H.; Park, H. Y.; Kim, K.; Suh, Y.-H.; Churchill, D. G. *Neurosci. Res.* **2011**, *71*, 168−177.
(28) Benesi, H. A.; Hildebrand, J. H. *J. Am. Chem. Soc.* **1949**, *71*, 2703−2707.
(29) (a) Traut, T. W. *Mol. Cell. Biochem.* **1994**, *140*, 1−22. (b) Barshop, B. A.; Adamson, D. T.; Vellom, D. C.; Rosen, F.; Epstein, B. L.; Seegmiller, J. E. *Anal. Biochem.* **1991**, *197*, 266−272. (c) Russell, R. G.; Bisaz, S.; Donath, A.; Morgan, D. B.; Fleisch, H. *J. Clin. Invest.* **1971**, *50*, 961−969.
(30) Thordarson, P. *Chem. Soc. Rev.* **2011**, *40*, 1305−1323.